Hindawi Publishing Corporation
Advances in Condensed Matter Physics
Volume 2014, Article ID 929750, 8 pages
http://dx.doi.org/10.1155/2014/929750

Research Article

First-Principles Study of the Structural Stability and Electronic and Elastic Properties of Helium in α-Zirconium

Jian Zheng,[1,2] Huijun Zhang,[2,3] Xiaosong Zhou,[2] Jianhua Liang,[2] Liusi Sheng,[1] and Shuming Peng[2]

[1] *School of Nuclear Science and Technology, University of Science and Technology of China, Hefei 230026, China*
[2] *Institute of Nuclear Physics and Chemistry, China Academy of Engineering Physics, Mianyang 621900, China*
[3] *School of Mathematics and Physics, University of Science and Technology Beijing, Beijing 100083, China*

Correspondence should be addressed to Shuming Peng; pengshuming@hotmail.com

Received 22 January 2014; Revised 11 April 2014; Accepted 20 April 2014; Published 5 May 2014

Academic Editor: Haiyan Xiao

First-principles calculations within density functional theory have been performed to investigate the behaviors of helium in α-zirconium. The most favorable interstitial site for He in α-Zr is not an ordinary tetrahedral or octahedral site, but a basal octahedral site with a formation energy as low as 2.40 eV. The formation energy reduces to 1.25 eV in the presence of preexisting vacancies. The analysis on the density of states and the charge density has been carried out. In addition, the influences of He and small He-V complexes on the elastic properties have been studied. The He-V complexes have been found to greatly affect the elastic properties compared with He alone.

1. Introduction

During service lifetime of materials used in nuclear energy systems, the impact of helium has been considered as a critical issue. Helium is almost insoluble in metals due to its inert reactivity with other elements. Once introduced, it can hardly be outgassed and will have profound deleterious effects on the microstructures and mechanical properties. Helium has been a topic of sustained interest during the past several decades for both nuclear material engineering and fundamental research. In particular, numerous experimental and theoretical studies have been dedicated to addressing the properties of He in metals such as Ti [1, 2], Fe [3, 4], and W [5, 6]. It is known to affect the nucleation and growth of voids in metals, causing noticeable dimensional changes and significant hardening [7–10].

Zirconium and its alloys are widely used in tritium storage [11–13] and nuclear fission energy systems [14–18] owing to their high tritium storage density, low thermal neutron absorption cross-section, good aqueous corrosion resistance, and favorable mechanical properties. And they are believed to have some potential uses in future fusion applications [19]. Under these application conditions, helium can be introduced by three principal ways: tritium β decay, (n, α) reactions, and direct He-ion implantation [20]. The tritium stored in zirconium can decay to helium by β decay in the following nuclear equation: ${}^{3}_{1}\mathrm{T} \rightarrow {}^{3}_{2}\mathrm{He}^{+} + \mathrm{e}^{-} + \bar{\nu}_e$. In fission reactors, because of the Ni doped in zirconium alloy and the B doped in the primary-loop water, the neutron flux may cause generation of helium either by (a) the two-step reaction with ${}^{58}\mathrm{Ni}(n, \gamma)$ and ${}^{59}\mathrm{Ni}(n, \gamma)$ or by (b) the ${}^{10}\mathrm{B} + \mathrm{n} \rightarrow {}^{7}\mathrm{Li} + \alpha$ reaction [21]. In fusion reactors, He^{++} and He^{+} ions produced in the plasma can directly implant into materials.

However, as far as we know, only a few studies have been centered on the influences of He on Zr, mainly some experimental works on the surface phenomenology [22, 23] and He bubble formation [12, 24]. It is found that helium can easily form bubbles and these bubbles preferentially distribute in grain boundaries and dislocations. For direct He-ion implantation, blisters, even exfoliations, are evident at a critical dose [22, 23].

The pioneering theoretical study by Koroteev et al. [25] gives us a better understanding on the structure stability and electronic properties of the Zr-He system. However,

Table 1: Experimental and calculated lattice constants (Å) for α-Zr.

	a	c/a
This work	3.231	1.600
PW91/PAW [30]	3.213	1.605
PW91/UPP [31]	3.23	1.604
PW91/UPP [32]	3.223	1.606
Exp. [33]	3.23	1.593

their calculations were performed in a rather small system containing only two Zr atoms and one He atom, which corresponds to an extremely high helium concentration. As we know, the stability of self-interstitial atom in α-Zr is strongly affected by the system size [26–29]. So, it is necessary to further their studies concerning a larger system size.

In the present paper, through first-principles calculations we reported helium's behavior in α-Zr by focusing on the relative stabilities of single He defects, the electronic properties of He atom, and its nearest-neighbor Zr (NN-Zr) atom. We also studied the changes of elastic properties due to the introduction of He atoms and vacancies.

2. Computational Method

The present calculations were carried out using CASTEP [39]. Ultrasoft pseudo potential (USPP) [40] with a consistent cutoff energy of 450 eV based on density functional theory (DFT) was used. The Perdew, Burke, and Ernzerhof (PBE) form [41] of generalized gradient approximation (GGA) was applied as the exchange-correlation potential since it has been suggested by Domain et al. [31] that GGA performs better than the local density approximation (LDA) to describe the exchange-correlation functional of Zr.

During the relaxations, the Brillouin zone (BZ) integration was achieved using a cold smearing scheme (Methfessel-Paxton), with a smearing of sigma = 0.1 eV. BZ sampling was performed using the Monkhorst-Pack scheme, with a k-point spacing as close as possible to 0.030 Å^{-1} (i.e., $4 \times 4 \times 3$ k-point meshes for a 36-atom supercell and $4 \times 4 \times 2$ k-point meshes for a 54-atom supercell). The supercells were optimized using the Broyden-Fletcher-Goldfarb-Shanno (BFGS) [42] algorithm allowing both atomic positions and the lattice parameters to relax. The energy convergence criterion for self-consistent calculations was set as 1×10^{-6} eV. The criteria for ionic energy minimization were set as energy derivative $<1 \times 10^{-5}$ eV/atom, forces on individual atoms <0.01 eV Å^{-1}, displacement of atoms derivative <0.001 Å, and stress component on cell <0.05 GPa. The criteria for the calculation of elastic constants were set as energy derivative $<2 \times 10^{-6}$ eV/atom, forces on individual atoms <0.006 eV Å^{-1}, and displacement of atoms derivative $<2 \times 10^{-4}$ Å. The parameters selected above ensure the convergence of formation energies within 0.001 eV/atom. Spin polarization is not considered in all the calculations for the sake of time; our future work will involve it.

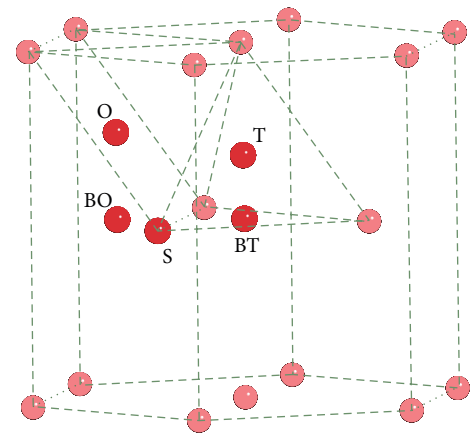

Figure 1: Five crystallographically unique interstitial sites in α-zirconium (hcp structure), where the pink spheres are the hcp lattice sites and the red ones are labeled as octahedral (O), basal octahedral (BO), tetrahedral (T), basal tetrahedral (BT), and substitutional (S) sites, respectively.

The defect formation energy is defined as

$$E^{f}_{\text{defect}} = E_{m\text{Zr,He}} - mE_{\text{Zr}} - E_{\text{He}}, \quad (1)$$

where $E_{m\text{Zr,He}}$ is the total energy of an optimized supercell containing m Zr atoms and one He atom, E_{Zr} is the energy per Zr atom in optimized crystal, and E_{He} is the energy of an isolated He atom.

3. Computational Results

3.1. Structural Stability. We first investigate the lattice constants of an α-Zr crystal and the results are summarized in Table 1, compared with experimental and other calculated results. It can be seen clearly that our calculated results are in good agreement with the corresponding experimental and other calculated values.

When He atoms are introduced into a metal, they may occupy either substitutional or interstitial lattice sites. It is necessary to figure out the locations of He atoms since they will influence the solubility and migration. It is also important for the understanding of such effects as damage trapping, bubble nucleation, embrittlement, and blistering [6]. It has been found that, in different metals, He atoms preferentially occupy different sites: substitutional sites for Fe, Cr, Mo, and W [6, 43], tetrahedral sites for Er [34], and FC (the center of equilateral trigonal face shared by two adjacent octahedrons) sites for Ti [2]. To identify the lowest energy configurations of the He interstitial defects in Zr and the possible influences of He concentration, supercells with 35 to 54 Zr atoms and one He atom were studied. Five crystallographically unique interstitial sites for He atom were taken into consideration (see Figure 1). They were denoted conventionally as octahedral (O), basal octahedral (BO), tetrahedral (T), basal tetrahedral (BT), and substitutional (S) sites.

The calculated formation energies of a single vacancy and He atom in above sites are listed in Table 2, together

Table 2: Vacancy formation energies (in eV) for a single He atom positioned in different sites. All the configurations are found to be stable, except O, which is unstable and transfers to BO. E_v^f represents the formation energy of a Zr vacancy and $E_s'^f$ represents the formation energy of a substitutional He atom in a preexisting Zr vacancy.

	E_v^f	E_s^f	$E_s'^f$	E_T^f	E_O^f	E_{BT}^f	E_{BO}^f
36-atom cell	1.97	3.30	1.33	2.67	/	3.01	2.42
54-atom cell	1.95	3.20	1.25	2.64	/	2.99	2.40
α-Zr [25]	—	—	—	3.08	3.19	—	—
Er [34]	—	2.59	—	1.73	1.98	—	—
Sc [35]	—	2.98	—	1.74	2.06	1.76	1.97
Ti [2]	—	3.65	1.70	2.82	3.04	—	2.69

with the results reported in the literature for Zr and some other hcp-structure metals. It is noticeable that, in both supercells, the configuration O is not stable and decays to configuration BO during relaxation. Different from those of Fe, Cr, Mo, and W, the favorable sites in energy for He atom in α-Zr are interstitial sites. Among the three stable interstitial sites, the most favorable one is the BO site in both supercells, with formation energy near 2.40 eV. However, it should be mentioned that E_s^f here actually represents the energy required to form a He-V complex. The formation energy of 1.33 eV for a He atom in a preexisting vacancy (denoted as $E_s'^f$) can be obtained by subtracting the formation energy of the vacancy (denoted as E_v^f). It is much smaller than E_{BO}^f, which means that He atoms can be trapped easily by preexisting vacancies. This is consistent with the case of Ti [2]. For materials used in nuclear systems, energetic particles like neutrons, ions, or electrons can induce significant microstructure alteration, especially the generation of large concentrations of vacancies, which can strongly affect the He distribution. In general, the stabilities of these configurations, in descending order, are preexisting vacancy, BO, T, BT, S, and O. Koroteev et al. [25] also reported that the configuration T is more stable than configuration O. However, they did not take other configurations into consideration. And maybe due to the differences in calculating methods or system sizes, their calculated configuration O does not decay to BO. This is left to be clarified by further studies.

3.2. Electronic Properties. To further understand the relative stability of these structures with He at various sites, we also studied the DOS of the He atoms and the NN-Zr atoms of different configurations. The relative stability of the He at BO site to the other sites can be easily understood according to the position of the Fermi level relative to the peaks in the DOS, which determines the occupation of the states and the nature of bonding [44]. As shown in Figure 2(a), the interaction of basal octahedral He interstitial with its NN-Zr atoms leads to the lowest DOS at the Fermi level which indicates that there is a stronger bonding between Zr atom and He atom at the BO site compared with other sites. This is in accordance with the formation energy differences as mentioned above. Different from those for Fe [43], it is also noticeable that the interaction also leads to different changes of the DOS at the Fermi level of the NN-Zr atoms, as shown in Figure 2(b). Comparing with that of the T and BT interstitial sites, the BO sites occupy a lower DOS at the Fermi level. The DOS at the Fermi level of the S site is somewhat particular because of the lack of one Zr atom. From Figure 3, we observe similar DOS peaks of the He-*s* and Zr-*d* states at around −1 eV and Fermi level, which suggests the strong hybridization between these states. And this hybridization between He and metals has also been confirmed by other researchers [34, 35, 43]. It is believed that the DOS peaks of the He-*s* and M- (metals-, like Zr, Sc, Er, Fe, etc.) *d* states will change due to the strong hybridization. This change will lead to an overall similarity in the shapes of those DOS curves.

We also calculated the total charge density ($\rho(r)$) of pure α-Zr crystal and one with preexisting vacancies. The isosurfaces of $\rho(r) = 140\,\mathrm{e/nm^3}$ and the contour plots of the charge density of the basal planes crossing the BO and S sites are illustrated in Figures 4(a) and 4(b), respectively. The isosurfaces are tubes similar to those of Ti [2]. Since the charge density inside the isosurfaces is lower than that of the outside, He atoms prefer to stay inside, especially in the BO or S sites, over which the tubes cross with the basal planes. It is obvious that the space inside the tube near the vacancy is much larger than that of the BO interstitial site. And this may explain why He atoms prefer to stay in preexisting vacancies.

3.3. Elastic Properties. Then, we studied the influences of helium on the elastic constants of Zr. For hexagonal structure materials, there are six elastic stiffness constants; five of them are independent (C_{11}, C_{12}, C_{13}, C_{33}, and C_{44}) with $C_{66} = (C_{11} - C_{12})/2$. The elastic constants were determined from the second derivatives of the total energy with respect to suitable deformations. The bulk modulus B and shear modulus G of the polycrystal were evaluated from the elastic constants of a single crystal by employing the Voigt-Reuss-Hill method [45–47]. For hexagonal lattices, the Reuss and Voigt bulk modulus (B_R and B_V) and the Reuss and Voigt shear (G_R and G_V) can be defined as [45–47]

$$
\begin{aligned}
B_R &= \frac{C_{33}\left(C_{11}+C_{12}\right)-2C_{13}^2}{C_{11}+C_{12}+2C_{33}-4C_{13}},\\
B_V &= \frac{1}{9}\left[2\left(C_{11}+C_{12}\right)+C_{33}+4C_{13}\right],\\
G_R &= \frac{5}{2}\frac{C_{44}C_{66}\left[C_{33}\left(C_{11}+C_{12}\right)-2C_{13}^2\right]}{3B_VC_{44}C_{66}+\left(C_{44}+C_{66}\right)\left[C_{33}\left(C_{11}+C_{12}\right)-2C_{13}^2\right]},\\
G_V &= \frac{1}{30}\left(C_{11}+C_{12}+2C_{33}-4C_{13}+12C_{44}+12C_{66}\right),\\
G &= \frac{1}{2}\left(G_R+G_V\right),\\
B &= \frac{1}{2}\left(B_R+B_V\right).
\end{aligned}
\tag{2}
$$

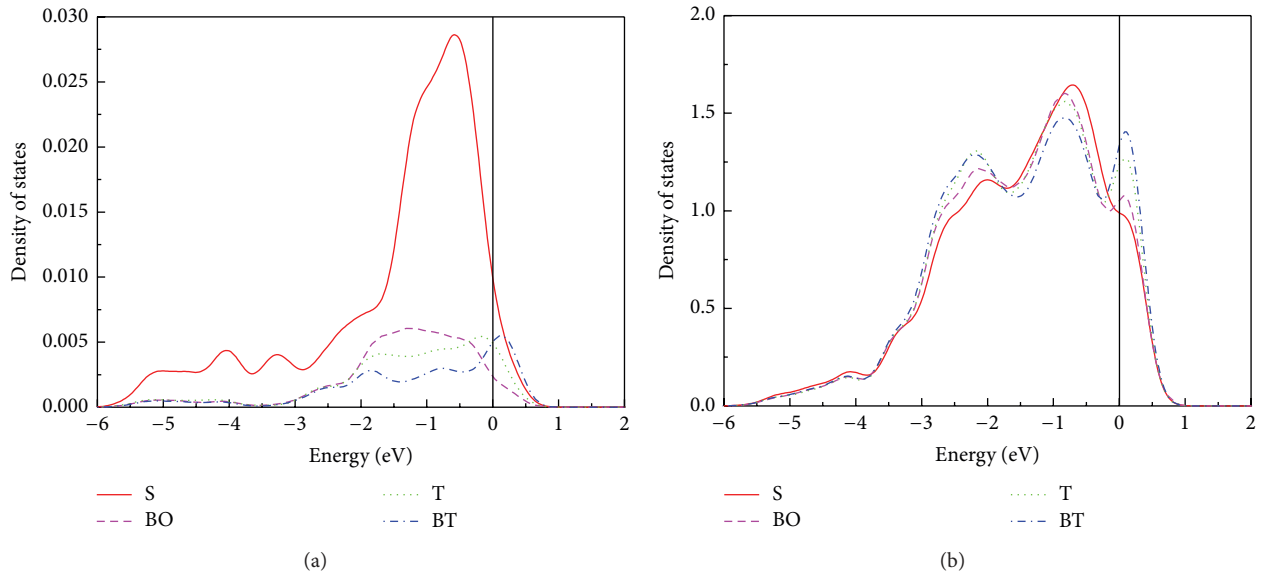

FIGURE 2: Total DOS of (a) an interstitial He atom at various positions and (b) its NN-Zr atoms (vertical line is the Fermi level E_F).

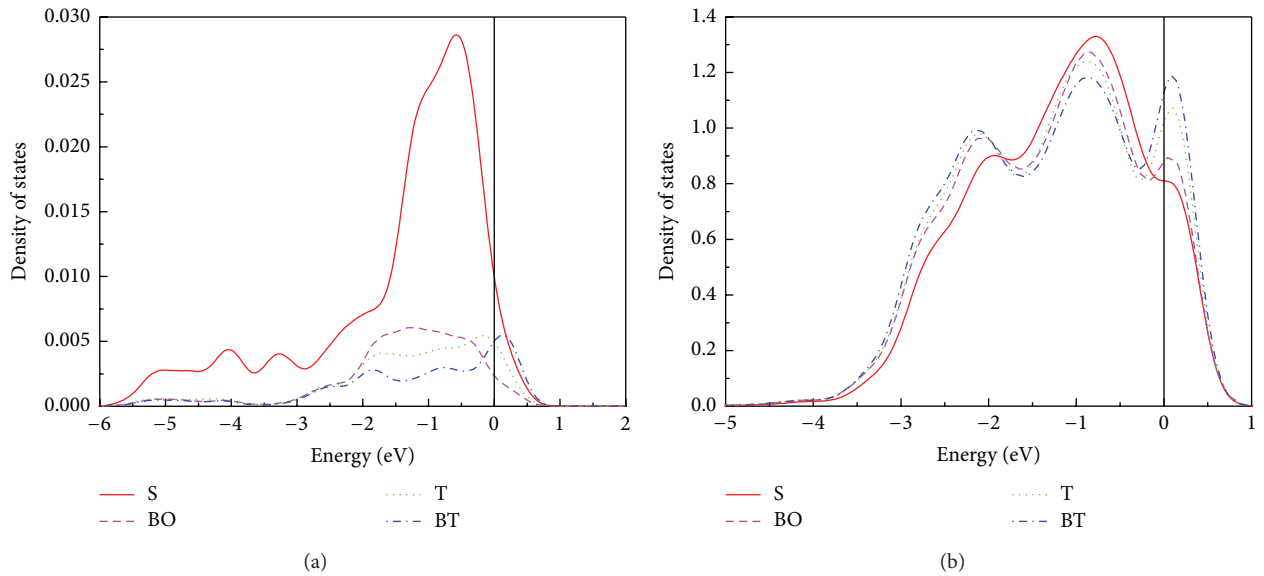

FIGURE 3: Local DOS of a He interstitial and its NN-Zr: (a) the *s*-projected DOS of He and (b) *d*-projected DOS of NN-Zr for the He interstitials at various positions (vertical line is the Fermi level E_F).

Using these values, Young's modulus E can be obtained by [37]

$$E = \frac{9BG}{3B + G}. \tag{3}$$

The elastic anisotropy is expressed by two popular anisotropic indexes, that is, the percentage anisotropy in shear (A_G) [48] and the universal anisotropic index (A^U) [49]. They are defined as

$$A_G = \frac{G_V - G_R}{G_V + G_R}, \qquad A^U = 5\frac{G_V}{G_R} + \frac{B_V}{B_R} - 6. \tag{4}$$

These values can range from zero (i.e., completely elastic isotropic) to 100% (i.e., the maximum anisotropic).

All of the calculated elastic constants results are listed in Table 3. For α-Zr, our calculated compressive moduli C_{11} and C_{33} and shear moduli C_{12} and C_{13} agree well with experimental results (at 298 K) showing an accuracy of about ±10%. However, our calculations underestimate the shear modulus C_{44} by about 21%. And these errors seem to also exist in others' reports [31]. There are at least two factors leading to these errors: one is the significance of temperature dependence [38], since first-principle calculations are all conducted at 0 K; the other one is the intrinsic feature of DFT calculations within the ultrasoft pseudo potentials

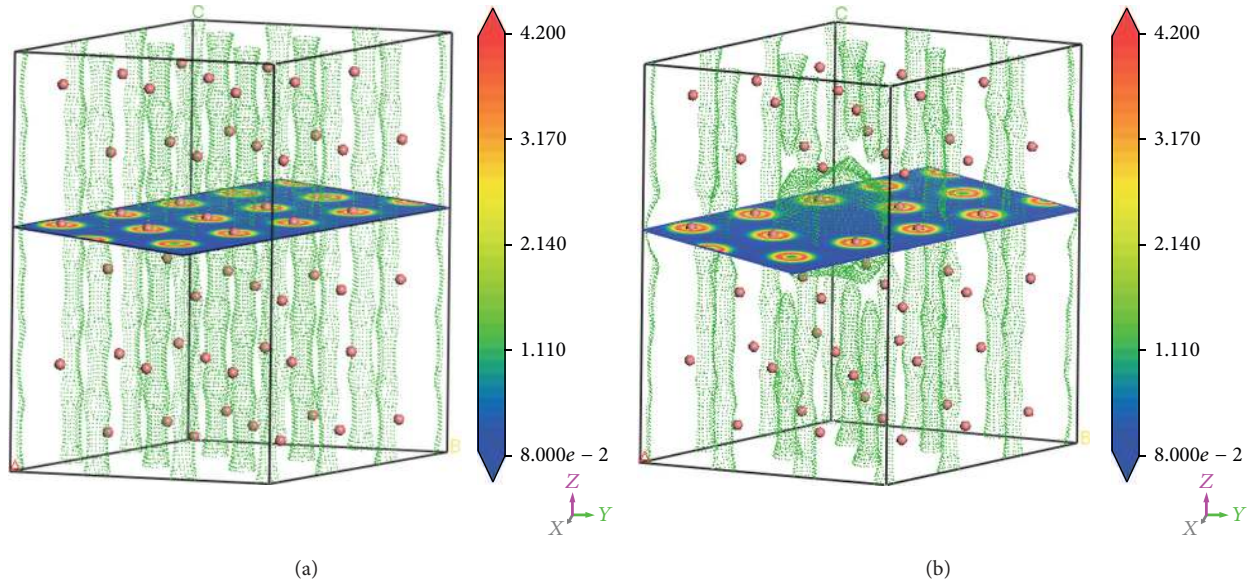

FIGURE 4: The charge density ($\rho(r)$) in a (a) perfect Zr crystal and (b) 54-atom Zr supercell with one Zr atom substituted by a vacancy. The green dotted surfaces are the isosurfaces of $\rho(r) = 140\,\mathrm{e/nm^3}$ and the slices are the contour plots of the charge density of the basal planes crossing the BO and S sites.

TABLE 3: Elastic constants C_{ij} (in GPa), bulk modulus B (in GPa), shear modulus G (in GPa), Young's modulus E (in GPa), percentage anisotropy in shear A_G, and universal anisotropic index A^U of α-Zr and Zr-He systems as calculated in the present work compared with experimental values.

	C_{11}	C_{33}	C_{12}	C_{13}	C_{44}	B	G	E	A_G	A^U
α-Zr (this work)	138.22	145.17	65.62	70.27	25.14	92.59	31.19	84.13	0.016	0.16
α-Zr (PBE/PAW) [36]	157	158	51	62	15	91	29	80		
α-Zr (PW91/UPP) [31]	142	164	64	64	29	92				
α-Zr (PW91/UPP) [32]	159.38	180.93	57.96	66.07	17.52	96.16	38.99	103.04		
α-Zr (PBE/UPP) [37]	139.4	162.7	71.3	66.3	25.5					
α-Zr (Exp.) [38] at 4 K	155.4	172.5	67.2	64.6	36.3					
α-Zr (Exp.) [38] at 298 K	143.4	164.8	72.8	65.3	32.0					
Zr96He (this work)	139.23	145.14	64.85	69.60	24.43	92.35	31.22	84.17	0.020	0.21
Zr54He (this work)	144.24	147.03	60.91	69.18	23.65	92.61	32.44	87.14	0.034	0.35
Zr36He (this work)	140.99	161.41	65.62	64.74	21.98	92.46	31.47	84.80	0.045	0.47

framework, which is involved in many approximations and simplifications for the sake of calculation time. Despite these errors from experimental values, first-principle methods are still considered to be efficient in calculating elastic constants [32, 37].

The differences of elastic constants between diagonal and off-diagonal elements for both α-Zr and Zr-He systems in Table 3 indicate their anisotropy to uniaxial compression and shear, biaxial compression, and distortion [32]. The addition of He atoms changes elastic constants in an anisotropic way: increasing C_{11} and decreasing C_{44} and C_{13}, while changing C_{12} and C_{33} in an irregular way. In particular, C_{44} and C_{13} change linearly with the He concentration. This elastic anisotropy can also be easily seen from the A_G and A^U values. Both indexes indicate that, with the increasing concentration of He, Zr host becomes more elastically anisotropic. Unfortunately, we failed to find any data on the effects of helium concentration on elastic constants in zirconium. Hence, we compared our results with those for hcp-Er [50], of which C_{11}, C_{33}, and C_{44} decrease and C_{12} increases linearly with He concentration, while C_{13} changes in an irregular way. This may be due to the crystal distortion caused by interstitial He atoms [50]. The changes of B, G, and E values in Table 3 are relatively small compared with those for Er [50]. According to the mechanical stability criteria for hexagonal phase, given by [51]

$$C_{44} > 0, \qquad C_{11} > |C_{12}|, \qquad (C_{11} + 2C_{12})\,C_{33} > 2C_{13}^2, \tag{5}$$

all of the systems we studied are still mechanically stable.

As mentioned above, large concentrations of vacancies can be generated in nuclear structural materials. So we also studied how the interactions between He and vacancies

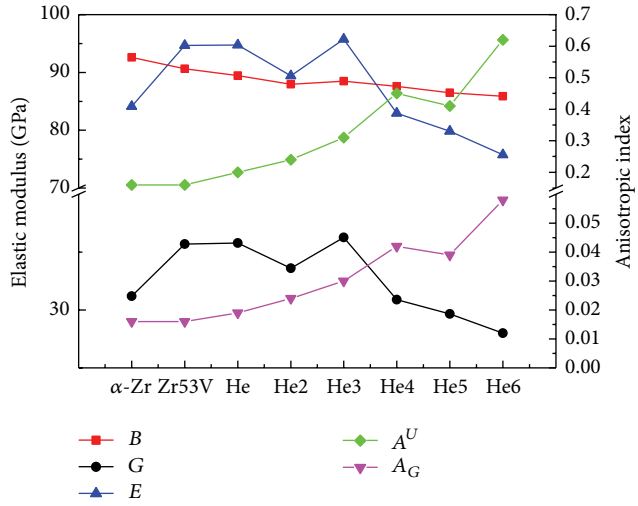

FIGURE 5: The elastic modulus (B, G, and E) and anisotropic index (A^U and A_G) of α-Zr and Zr-V-He systems calculated from Table 4 (He, He2... represent Zr53VHe, Zr53VHe2..., resp.).

TABLE 4: Elastic constants C_{ij} (in GPa) of α-Zr and Zr-V-He systems.

	C_{11}	C_{33}	C_{12}	C_{13}	C_{44}
α-Zr	138.22	145.17	65.62	70.27	25.14
Zr53V	143.05	149.01	58.64	66.04	28.81
Zr53VHe	143.77	145.08	56.57	64.92	28.35
Zr53VHe2	140.19	143.75	59.50	62.12	25.75
Zr53VHe3	144.53	153.28	55.23	61.13	26.91
Zr53VHe4	136.59	148.77	59.81	61.94	21.63
Zr53VHe5	133.72	144.20	61.79	60.91	21.08
Zr53VHe6	130.54	151.16	62.97	58.95	18.63

affect the elastic properties. Supercells with 53 Zr atoms, one vacancy, and several He atoms (0~6) were studied. The results are shown in Table 4 and Figure 5. Firstly, when a Zr atom in a 54-atom supercell is replaced by a vacancy, the elastic anisotropy does not change according to the A_G and A^U values while the C_{11}, C_{33}, and C_{44} values increase and the C_{12} and C_{13} values decrease. The evaluated B value of the polycrystal also decreases a little, in contrast to that of the G and E. When more He atoms are added to the vacancy, the elastic anisotropy increases linearly and significantly. At the same time, the elastic moduli C_{11}, C_{13}, and C_{44} decrease almost linearly with the increase in the He concentration, while C_{33} and C_{12} change irregularly. The B, G, and E values also decrease linearly with the increase in the He concentration, which is consistent with the case of Er [50]. Comparing with the single effect of He, the He-V complexes have affected the mechanical properties much more obviously. It seems that the presence of He-V clusters can lead to a significant deterioration of the mechanical properties of Zr, which may intensively limit their performances. In our future work, we will promote our study by considering the synergistic effects of He and H on Zr, since these two elements always cooperate with each other in nuclear environment, producing strengthened effects on nuclear materials.

4. Conclusion

In the present study, first-principles calculation has been conducted to investigate the structural stability and electronic and mechanical properties of Zr-He systems. For the perfect α-Zr crystal, the He BO interstitial site is most energetically favorable, while, for a not perfect one with preexisting vacancies, the S site is most stable. The analysis on the DOS and charge density gives a better understanding about the structural stability issue. It is found that the introduction of He changes the elastic constants in an anisotropic way, leading to a significant increase in elastic anisotropy. And this effect is further enlarged while He-V complexes form, resulting in an intensive deterioration of the mechanical properties of Zr.

Conflict of Interests

The authors declare that there is no conflict of interests regarding the publication of this paper.

Acknowledgments

The authors are very grateful for the financial support by the Science Foundation of China Academy of Engineering Physics, China (Grant no. 2010A0301011), and by the National Natural Science Foundation of China (Grant no. 91126001).

References

[1] T. Schober and K. Farrell, "Helium bubbles in α-Ti and Ti tritide arising from tritium decay: a tem study," *Journal of Nuclear Materials*, vol. 168, no. 1-2, pp. 171–177, 1989.

[2] Y.-L. Wang, S. Liu, L.-J. Rong, and Y.-M. Wang, "Atomistic properties of helium in hcp titanium: a first-principles study," *Journal of Nuclear Materials*, 2010.

[3] D. Xu, T. Bus, S. C. Glade, and B. D. Wirth, "Thermal helium desorption spectrometry of helium-implanted iron," *Journal of Nuclear Materials*, vol. 367–370, pp. 483–488, 2007.

[4] S. J. Zenobia, L. M. Garrison, and G. L. Kulcinski, "The response of polycrystalline tungsten to 30 keV helium ion implantation at normal incidence and high temperatures," *Journal of Nuclear Materials*, vol. 425, no. 1–3, pp. 83–92, 2012.

[5] E. V. Kornelsen and A. A. Van Gorkum, "Study of bubble nucleation in tungsten using thermal desorptionspectrometry: clusters of 2 to 100 helium atoms," *Journal of Nuclear Materials*, vol. 92, no. 1, pp. 79–88, 1980.

[6] C. S. Becquart and C. Domain, "Migration energy of He in W revisited by Ab initio calculations," *Physical Review Letters*, vol. 97, no. 19, Article ID 196402, 2006.

[7] R. L. Simons, H. R. Brager, and W. Y. Matsumoto, "Design of a single variable helium effects experiment for irradiation in FFTF using alloys enriched in nickel-59," *Journal of Nuclear Materials*, vol. 141–143, no. 2, pp. 1057–1060, 1986.

[8] T. Ishizaki, Q. Xu, T. Yoshiie, S. Nagata, and T. Troev, "The effect of hydrogen and helium on microvoid formation in iron and

nickel," *Journal of Nuclear Materials*, vol. 307–311, no. 2, pp. 961–965, 2002.

[9] J. D. Hunn, E. H. Lee, T. S. Byun, and L. K. Mansur, "Helium and hydrogen induced hardening in 316LN stainless steel," *Journal of Nuclear Materials*, vol. 282, no. 2-3, pp. 131–136, 2000.

[10] N. Sekimura, T. Iwai, Y. Arai et al., "Synergistic effects of hydrogen and helium on microstructural evolution in vanadium alloys by triple ion beam irradiation," *Journal of Nuclear Materials*, vol. 283–287, pp. 224–228, 2000.

[11] T. Schober, H. Trinkaus, and R. Lässer, "A TEM study of the aging of Zr tritides," *Journal of Nuclear Materials*, vol. 141–143, no. 1, pp. 453–457, 1986.

[12] T. Schober and R. Lässer, "The aging of zirconium tritides: a transmission electron microscopy study," *Journal of Nuclear Materials*, vol. 120, no. 2-3, pp. 137–142, 1984.

[13] T. Hayashi, T. Suzuki, and K. Okuno, "Long-term measurement of helium-3 release behavior from zirconium-cobalt tritide," *Journal of Nuclear Materials*, vol. 212–215, pp. 1431–1435, 1994.

[14] B. Cox, "Pellet-clad interaction (PCI) failures of zirconium alloy fuel cladding—a review," *Journal of Nuclear Materials*, vol. 172, no. 3, pp. 249–292, 1990.

[15] B. A. Cheadle, C. E. Ells, and W. Evans, "The development of texture in zirconium alloy tubes," *Journal of Nuclear Materials*, vol. 23, no. 2, pp. 199–208, 1967.

[16] A. Yilmazbayhan, A. T. Motta, R. J. Comstock, G. P. Sabol, B. Lai, and Z. Cai, "Structure of zirconium alloy oxides formed in pure water studied with synchrotron radiation and optical microscopy: relation to corrosion rate," *Journal of Nuclear Materials*, vol. 324, no. 1, pp. 6–22, 2004.

[17] R. N. Singh, A. K. Bind, N. S. Srinivasan et al., "Influence of hydrogen content on fracture toughness of CWSR Zr-2.5 Nb pressure tube alloy," *Journal of Nuclear Materials*, vol. 432, no. 1, pp. 87–93, 2012.

[18] S. C. Lumley, S. T. Murphy, P. A. Burr et al., "The stability of alloying additions in Zirconium," *Journal of Nuclear Materials*, vol. 437, no. 1, pp. 122–129, 2013.

[19] C. B. A. Forty and P. J. Karditsas, "Uses of zirconium alloys in fusion applications," *Journal of Nuclear Materials*, vol. 283–287, pp. 607–610, 2000.

[20] A. A. Lucas, "Helium in metals," *Physica B: Physics of Condensed Matter*, vol. 127, no. 1–3, pp. 225–239, 1984.

[21] Y. Dai, G. R. Odette, and T. Yamamoto, "The effects of helium in irradiated structural alloys," in *Comprehensive Nuclear Materials*, pp. 141–193, Elsevier, 2012.

[22] D. K. Sood, M. Sundararaman, S. K. Deb, R. Krishnan, and M. K. Mehta, "Blistering of zirconium, inconel-718 and stainless steel-316 by 2 MeV helium ions," *Journal of Nuclear Materials*, vol. 79, no. 2, pp. 423–425, 1979.

[23] R. H. Zee, J. F. Watters, and O. M. Westcott, "On the critical dose for blistering in helium irradiated zirconium and ZrNb," *Journal of Nuclear Materials*, vol. 115, no. 1, pp. 131–133, 1983.

[24] H. Zheng, S. Liu, H. B. Yu, L. B. Wang, C. Z. Liu, and L. Q. Shi, "Introduction of helium into metals by magnetron sputtering deposition method," *Materials Letters*, vol. 59, no. 8-9, pp. 1071–1075, 2005.

[25] Y. M. Koroteev, O. V. Lopatina, and I. P. Chernov, "Structure stability and electronic properties of the Zr-He system: first-principles calculations," *Physics of the Solid State*, vol. 51, no. 8, pp. 1600–1607, 2009.

[26] Q. Peng, W. Ji, H. Huang et al., "Stability of self-interstitial atoms in hcp-Zr," *Journal of Nuclear Materials*, vol. 429, no. 1, pp. 233–236, 2012.

[27] Q. Peng, W. Ji, H. Huang et al., "Axial ratio dependence of the stability of self-interstitials in HCP structures," *Journal of Nuclear Materials*, vol. 437, no. 1, pp. 293–296, 2013.

[28] G. D. Samolyuk, S. I. Golubov, Y. N. Osetsky et al., "Self-interstitial configurations in hcp Zr: a first principles analysis," *Philosophical Magazine Letters*, vol. 93, no. 2, pp. 93–100, 2013.

[29] G. Vérité, C. Domain, C. C. Fu et al., "Self-interstitial defects in hexagonal close packed metals revisited: evidence for low-symmetry configurations in Ti, Zr, and Hf," *Physical Review B*, vol. 87, no. 13, Article ID 134108, 2013.

[30] F. Wang and H. R. Gong, "First principles study of various Zr-H phases with low H concentrations," *International Journal of Hydrogen Energy*, vol. 37, no. 17, pp. 12393–12401, 2012.

[31] C. Domain, R. Besson, and A. Legris, "Atomic-scale Ab-initio study of the Zr-H system: I. Bulk properties," *Acta Materialia*, vol. 50, no. 13, pp. 3513–3526, 2002.

[32] W. Zhu, R. Wang, G. Shu, P. Wu, and H. Xiao, "First-principles study of different polymorphs of crystalline zirconium hydride," *Journal of Physical Chemistry C*, vol. 114, no. 50, pp. 22361–22368, 2010.

[33] S. K. Sikka, Y. K. Vohra, and R. Chidambaram, "Omega phase in materials," *Progress in Materials Science*, vol. 27, no. 3-4, pp. 245–310, 1982.

[34] L. Yang, S. M. Peng, X. G. Long et al., "Ab initio study of intrinsic, H, and He point defects in hcp-Er," *Journal of Applied Physics*, vol. 107, no. 5, Article ID 054903, 2010.

[35] L. Yang, S. M. Peng, X. G. Long et al., "Ab initio study of stability and migration of H and He in hcp-Sc," *Journal of Physics Condensed Matter*, vol. 23, no. 3, Article ID 035701, 2011.

[36] J. Blomqvist, J. Olofsson, A. M. Alvarez et al., "Structure and thermodynamical Properties of Zirconium hydrides from first-principle," in *Proceedings of the 15th International Conference on Environmental Degradation of Materials in Nuclear Power Systems-Water Reactors*, 2012.

[37] H. Ikehata, N. Nagasako, T. Furuta, A. Fukumoto, K. Miwa, and T. Saito, "First-principles calculations for development of low elastic modulus Ti alloys," *Physical Review B—Condensed Matter and Materials Physics*, vol. 70, no. 17, Article ID 174113, 2004.

[38] E. S. Fisher and C. J. Renken, "Single-crystal elastic moduli and the hcp → bcc transformation in Ti, Zr, and Hf," *Physical Review*, vol. 135, no. 2A, article A482, 1964.

[39] S. J. Clark, M. D. Segall, C. J. Pickard et al., "First principles methods using CASTEP," *Zeitschrift fur Kristallographie*, vol. 220, no. 5-6, pp. 567–570, 2005.

[40] D. Vanderbilt, "Soft self-consistent pseudopotentials in a generalized eigenvalue formalism," *Physical Review B*, vol. 41, no. 11, article 7892, 1990.

[41] J. P. Perdew, K. Burke, and M. Ernzerhof, "Generalized gradient approximation made simple," *Physical Review Letters*, vol. 77, no. 18, article 3865, 1996.

[42] B. G. Pfrommer, M. Côté, S. G. Louie, and M. L. Cohen, "Relaxation of crystals with the Quasi-Newton method," *Journal of Computational Physics*, vol. 131, no. 1, pp. 233–240, 1997.

[43] X. T. Zu, L. Yang, F. Gao et al., "Properties of helium defects in bcc and fcc metals investigated with density functional theory," *Physical Review B—Condensed Matter and Materials Physics*, vol. 80, no. 5, Article ID 054104, 2009.

[44] R. Pentcheva and M. Scheffler, "Initial adsorption of Co on Cu(001): a first-principles investigation," *Physical Review B—Condensed Matter and Materials Physics*, vol. 65, no. 15, Article ID 155418, 2002.

[45] W. Voigt, *Lehrbuch der Kristallphysik*, Teubner, Leipzig, Germany, 1928.

[46] A. Reuss and Z. Angnew, "A calculation of the bulk modulus of polycrystalline materials," *Mathematical Methods*, vol. 9, article 55, 1929.

[47] R. Hill, "The elastic behaviour of a crystalline aggregate," *Proceedings of the Physical Society A*, vol. 65, no. 5, article 349, 1952.

[48] D. H. Chung, W. R. Buessem, F. W. Vahldiek et al., *Anisotropy in Single Crystal Refractory Compounds*, Plenum Press, New York, NY, USA, 1968.

[49] S. I. Ranganathan and M. Ostoja-Starzewski, "Universal elastic anisotropy index," *Physical Review Letters*, vol. 101, no. 5, Article ID 055504, 2008.

[50] F. Kai-Min, Y. Li, S. Qing-Qiang et al., "First-principles study on elastic properties of hexagonal phase ErAx (A= H, He)," *Acta Physica Sinica*, vol. 62, no. 11, Article ID 116201, 2013.

[51] Z.-J. Wu, E.-J. Zhao, H.-P. Xiang, X.-F. Hao, X.-J. Liu, and J. Meng, "Crystal structures and elastic properties of superhard Ir N_2 and Ir N_3 from first principles," *Physical Review B—Condensed Matter and Materials Physics*, vol. 76, no. 5, Article ID 054115, 2007.